JOURNAL OF MATERIALS SCIENCE 31 (1996) 4407–4413

Effect of atmosphere on pyrolysis of Nicalon

TOSHIO SHIMOO, KIYOHITO OKAMURA
Department of Metallurgy and Materials Science, College of Engineering, University of Osaka Prefecture, Gakuen-cho, Sakai-shi, Osaka-fu 593, Japan

TOSHIHIDE HAYATSU
Graduate Student, University of Osaka Prefecture, Gakuen-cho, Sakai-shi, Osaka-fu 593, Japan

The pyrolytic behaviour of Nicalon under a N_2 atmosphere was investigated at temperatures from 1673 to 1973 K, and was compared with that under an Ar atmosphere. The pyrolytic rate was measured by thermogravimetry, and heat-treated Nicalon was examined by X-ray diffraction, scanning electron microscopy, Auger electron spectroscopy and tensile testing. The pyrolytic rate was smaller in N_2 than in Ar. The nitrided case retarded the crystallization into β-SiC and retained its high strength. The effectiveness of the nitrided case disappeared on heating in Ar. The strength was related to the size of the β-SiC crystal in Nicalon.

1. Introduction

Polymer-derived SiC fibres have been used as reinforcing fibres for metal- and ceramic-base composites. Si–C–O (Nicalon, Nippon Carbon) and Si–Ti–C–O (Tyranno, Ube Industries) fibres are produced commercially, and then the low oxygen fibres are prepared as trial products using an irradiation-curing method. On heating at higher temperatures, all these fibres, which are amorphous and contain oxygen, crystallize to β-SiC while accompanied by the evolution of SiO and CO. This pyrolysis significantly reduces the strength of the fibre. Therefore, information on the thermochemical stability of these fibres is necessary to broaden their utilization as high-temperature materials. Many investigators have worked on the changes in microstructure and mechanical properties of the SiC fibres in various environments including air, Ar, N_2, O_2 and vacuum, and at various temperatures and pressures [1–7]. However, the pyrolytic kinetics of the fibres has not been fully investigated. So far, the authors have reported the pyrolytic mechanism of the polymer-derived fibre under an Ar or an O_2 atmosphere [8–14]. In the present work, the pyrolytic behaviour of Nicalon was studied under a N_2 atmosphere and were compared with that under an Ar atmosphere.

2. Experimental procedure

The SiC fibre used in this experiment is Nicalon NL202 (produced by Nippon Carbon Co. Ltd.) which is derived from polycarbosilane. This fibre has the molar composition of $SiC_{1.20}O_{0.41}$ and mean diameter of 15 μm. Nicalon was heated in Ar at 1073 K for 3.6 ks in order to remove the sizing agent prior to measurement.

The thermobalance unit used for thermogravimetry (TG) was composed of an analogue-type automatic recording balance and a carbon resistance furnace. The experimental temperature was measured with a 6%Rh/Pt–30%Rh/Pt thermocouple positioned close to the sample. N_2 was allowed to flow from the bottom of the furnace at a flow rate of $2.5 \times 10^{-5}\ m^3\ s^{-1}$. Fibres, 1 g in mass and 3 cm in length, were placed in a carbon crucible 26 mm in inner diameter and 50 mm in depth. The carbon crucible was suspended in the hot zone of the furnace with a graphite rod and a stainless steel wire acting as a balance. The mass loss was recorded automatically during each experiment. Upon completion of thermogravimetry, the fibres were cooled rapidly by raising the crucible to the low-temperature zone of the furnace. The pyrolysis products were identified by X-ray diffraction (XRD) and Auger electron spectroscopy (AES), and the morphology of the fibres was observed by scanning electron microscopy (SEM). Furthermore, the tensile strength of the fibres was measured at room temperature in the following manner. Using a load cell with 100 g full scale range, tensile testing of a monofilament of 10 mm gauge length was carried out on a Tensilon-type machine (Toyo Measuring Instrument Co. Type UTM-II-20) at a crosshead speed of $3.33 \times 10^{-2}\ mm\ s^{-1}$.

3. Results

3.1. TG curves

Nicalon was isothermally heated at temperatures from 1673 to 1973 K under an Ar or a N_2 atmosphere. Fig. 1 shows the TG curves. ΔW is the mass loss determined by a thermobalance and W_0 is the initial mass of Nicalon. The mass loss is due to the generation of both SiO and CO. The pyrolytic rates are smaller in N_2 than in Ar. In particular, the pyrolysis is markedly suppressed in N_2 below 1773 K. Additionally the final mass loss after completion of the pyrolysis is smaller in N_2 than in Ar.

0022–2461

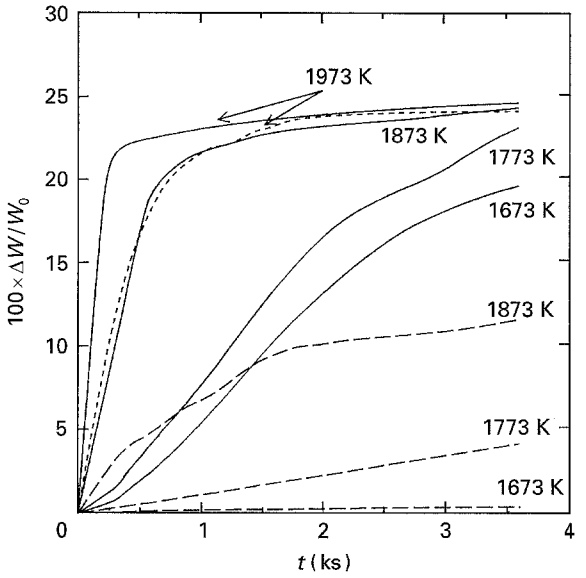

Figure 1 Mass loss of Nicalon heated in N_2 and Ar at various temperatures. Key: —— in Ar; – – – – in N_2.

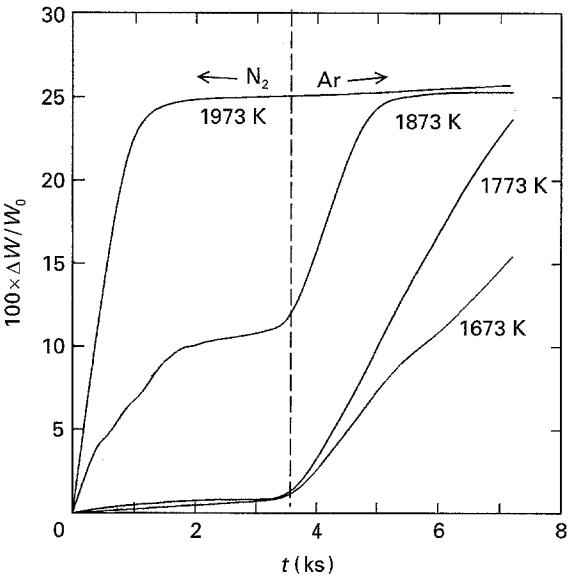

Figure 2 Mass loss of Nicalon heated in Ar after heating in N_2 at various temperatures.

In order to clarify the effect of atmosphere on the pyrolysis, Nicalon, which was heat-treated in N_2 for 3.6 ks, was successively heated in Ar for 3.6 ks at temperatures from 1673 to 1973 K. TG curves are shown in Fig. 2. Below 1873 K, the change of atmosphere from N_2 to Ar results in severe pyrolysis of Nicalon. At 1973 K, the mass remains unchanged under an Ar atmosphere, since the pyrolysis is completed before changing from N_2 to Ar.

3.2. X-ray diffraction

The X-ray diffraction patterns of Nicalon heated under different atmospheres at 1673, 1773, 1873 and 1973 K are shown in Figs 3–6, respectively. At 1673 K,

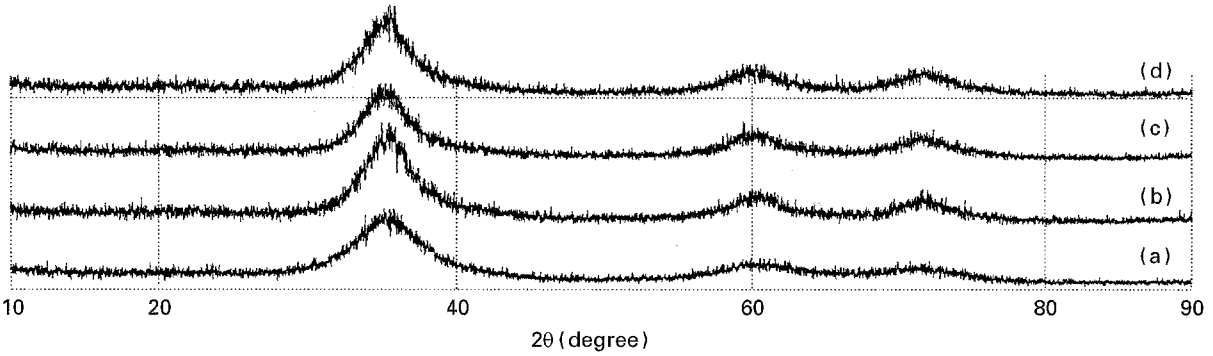

Figure 3 X-ray diffraction patterns of (a) original Nicalon, and (b) Nicalon heated in N_2, (c) in Ar after heating in N_2 and (d) in Ar at 1673 K.

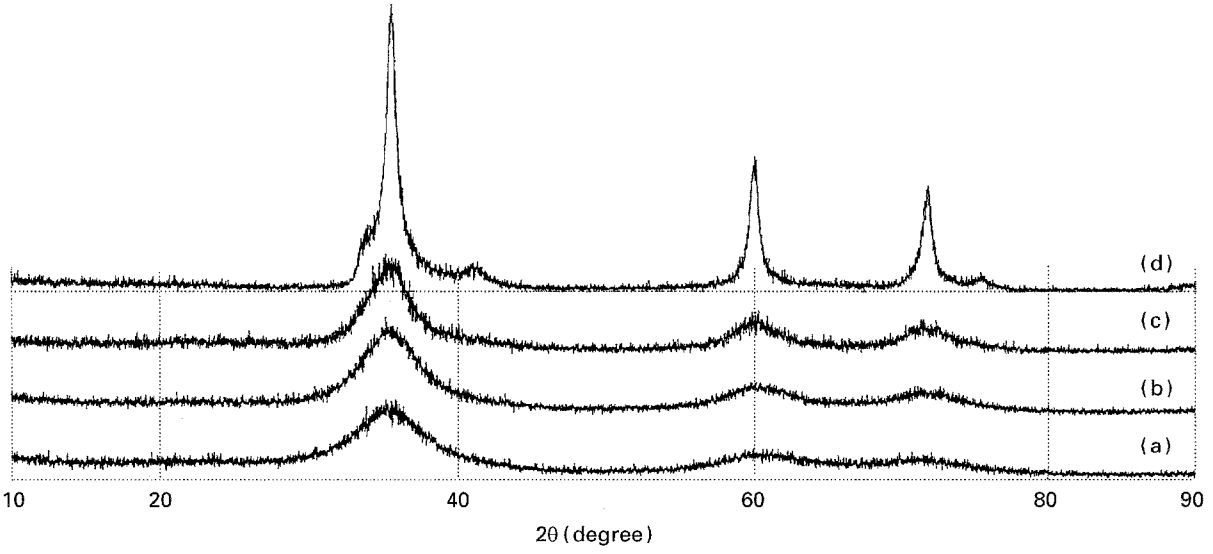

Figure 4 X-ray diffraction patterns of (a) original Nicalon, and (b) Nicalon heated in N_2, (c) in Ar after heating in N_2 and (d) in Ar at 1773 K.

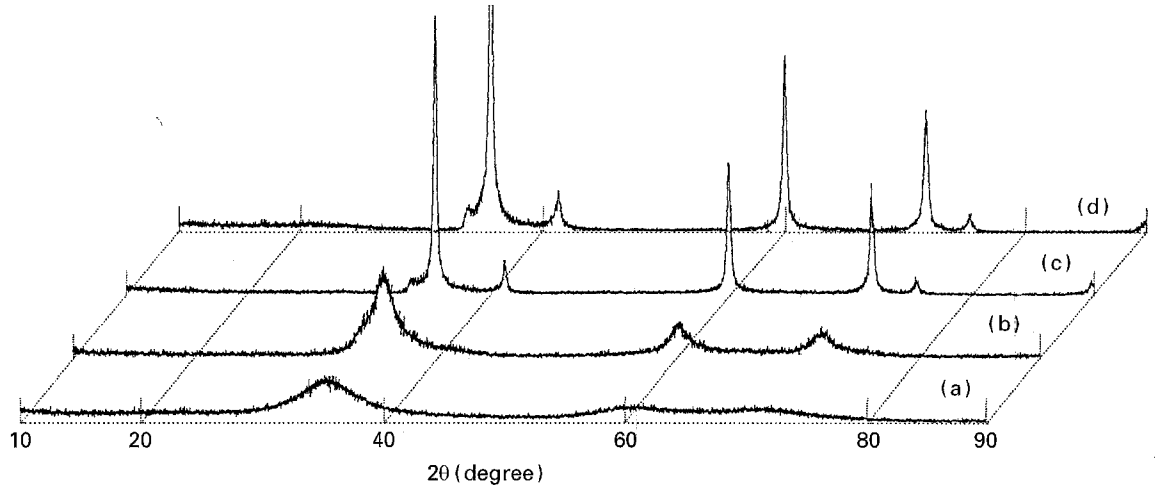

Figure 5 X-ray diffraction patterns of (a) original Nicalon, and (b) Nicalon heated in N_2, (c) in Ar after heating in N_2 and (d) in Ar at 1873 K.

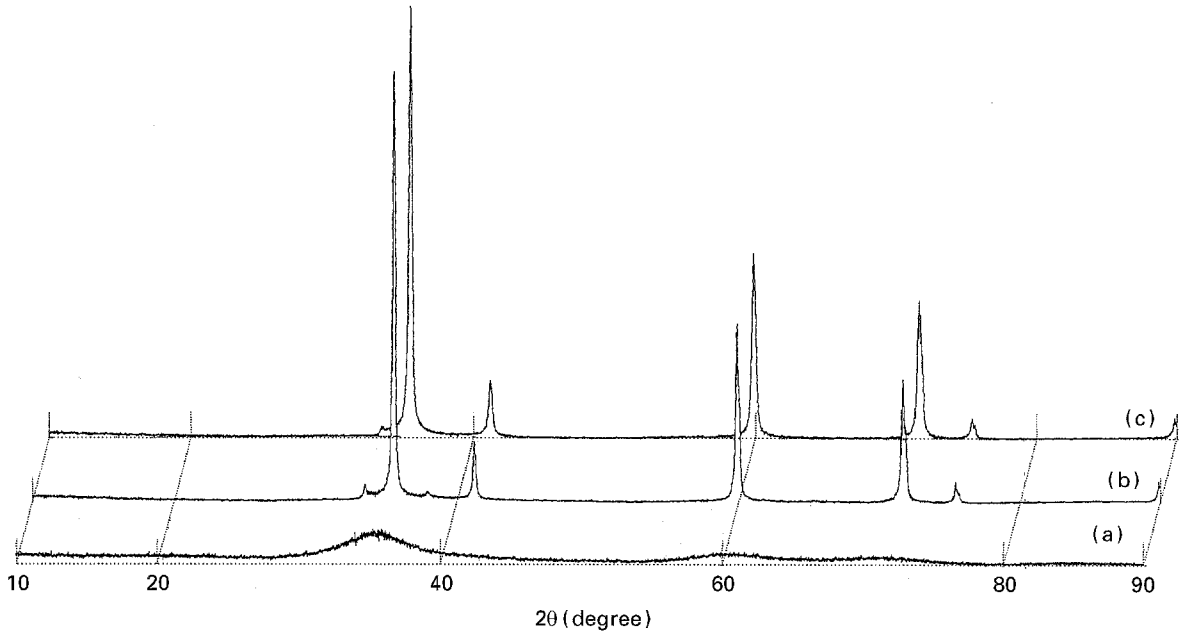

Figure 6 X-ray diffraction patterns of (a) original Nicalon, and (b) Nicalon heated in N_2 and (c) in Ar at 1973 K.

all heat-treated Nicalons have a broad diffraction pattern and are microcrystalline. At 1773 K, the diffraction pattern of Nicalon heat treated in Ar is sharp. However, the diffraction pattern of Nicalon previously heat treated in N_2 still remains broad after heating in Ar. As stated later, a nitrided case is formed by the heat treatment in N_2, and this is considered to suppress the pyrolysis of the core. At 1873 K, Nicalon remains microcrystalline in N_2, although it crystallizes greatly in Ar. However, the subsequent heat treatment in Ar leads to crystallization into β-SiC. Furthermore, Nicalon pyrolizes seriously even in N_2 at 1973 K. Thus, X-ray diffraction suggests that the effect of the nitridation on the pyrolysis of Nicalon is lost at high temperatures.

3.3. SEM observation

Fig. 7 shows the morphologies of the surface and the cross-section of Nicalon heated at 1873 K. The fibre heated in N_2 is smooth and featureless at SEM resolutions (Fig. 7a and b). The appearance of the fibre heat treated in Ar is coarse because of severe pyrolysis (Fig. 7c and d). Furthermore, the fibre heated in N_2 and subsequently in Ar has two layers: a coarse-grained case and a fine-grained core (Fig. 7e and f).

3.4. Tensile test

Fig. 8 shows the tensile strength of Nicalon as a function of heating temperature. The tensile strength

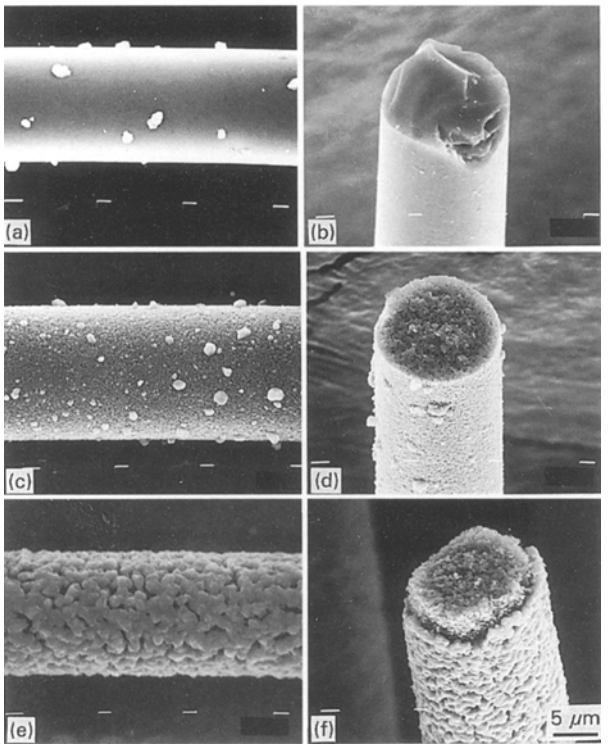

Figure 7 SEM photographs of Nicalon heated (a) and (b) in N_2 for 3.6 ks (c) and (d) in Ar for 3.6 ks, (e) and (f) and in Ar for 3.6 ks after heating in N_2 for 3.6 ks at 1873 K.

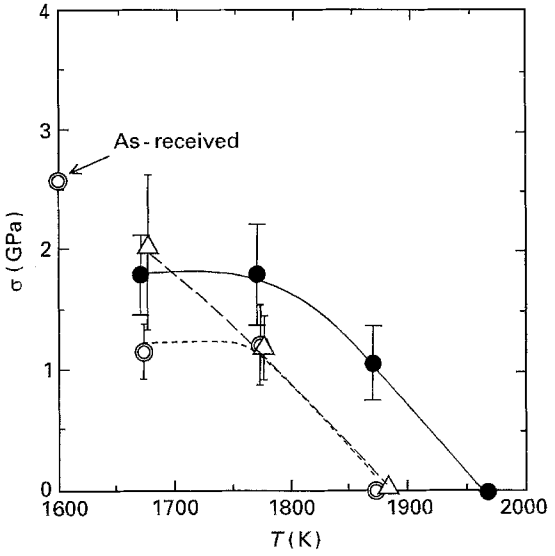

Figure 8 Tensile strength of Nicalon heated in N_2 for 3.6 ks (●), in Ar for 3.6 ks (◎) and in Ar for 3.6 ks after heating in N_2 for 3.6 ks (△) as function of temperature.

decreases with increasing temperature. At 1873 K, Nicalon heat treated in N_2 retains 42% of its original strength, while Nicalon heat treated in Ar loses all its strength. Below 1873 K, Nicalon heated in N_2 is stronger than Nicalon heat treated in Ar. On changing from N_2 to Ar, the strength does not change at 1673 K, but decreases to the same level for Nicalon heat treated only in Ar at 1773 and 1873 K.

3.5. AES analysis

Figs 9 to 12 present depth profiles of Nicalon. The as-received fibre has a thin oxide layer on the surface (Fig. 9). After heat treatment in Ar, oxygen was depleted as a consequence of the pyrolysis (Fig. 10). The fibre treated in N_2 exhibits a depth profile indicating that nitrogen is picked up on the surface (Fig. 11). Even after being heated subsequently in Ar, considerable nitrogen is retained in Nicalon (Fig. 12). The nitrided case is considered to be formed on the fibre and to suppress the pyrolysis. Consequently, there is a slight amount of oxygen in the fibre treated in N_2. The oxygen-rich surface of the fibre treated subsequently in Ar (Fig. 12) is probably due to exposure in air after the heat treatment.

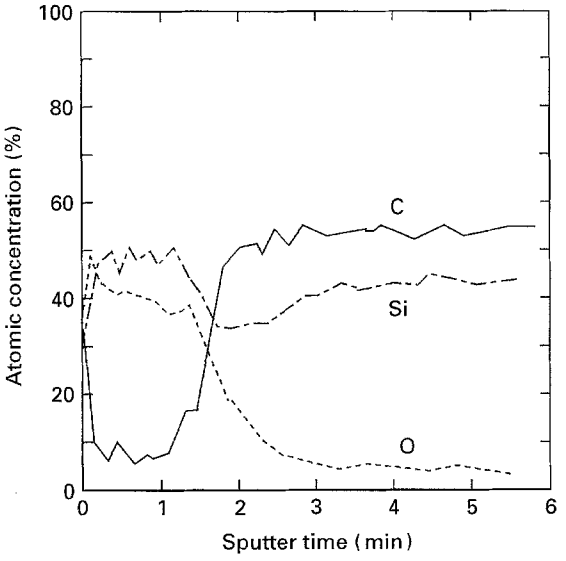

Figure 9 AES depth profile of as-received Nicalon (sputter-rate 14 nm min^{-1}: SiO_2).

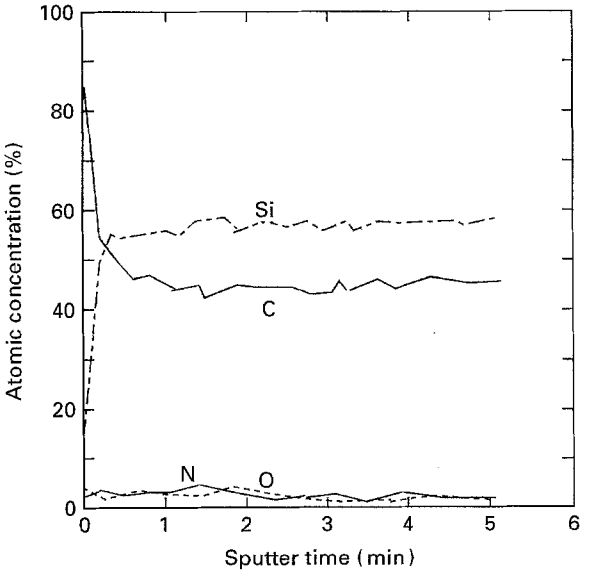

Figure 10 AES depth profile of Nicalon heated in Ar for 3.6 ks at 1873 K (sputter rate 14 nm min^{-1}: SiO_2).

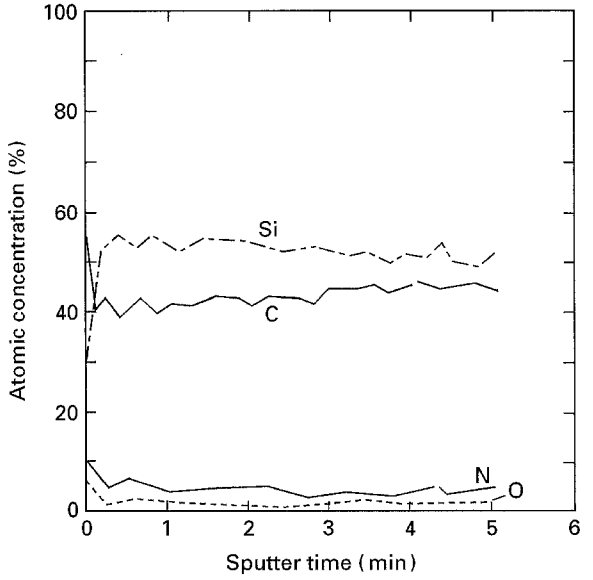

Figure 11 AES depth profile of Nicalon heated in N_2 for 3.6 ks at 1873 K (sputter rate 14 nm min^{-1}: SiO_2).

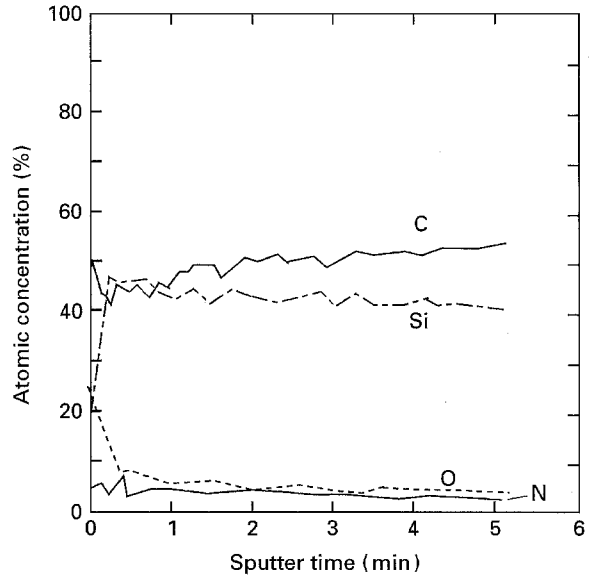

Figure 12 AES depth profile of Nicalon heated in Ar for 3.6 ks after heating in N_2 for 3.6 ks at 1873 K (sputter rate 14 nm min^{-1}: SiO_2).

4. Discussion

Previously, the pyrolytic mechanism of Nicalon was investigated under an Ar atmosphere [8, 9, 12]. The pyrolysis leads to the crystallization of amorphous fibre into β-SiC, involving the generation of both SiO and CO gases.

$$SiC_{1.20}O_{0.41}(s) = 0.895SiC(s) + 0.105SiO(g) + 0.305CO(g) \quad (1)$$

This pyrolysis proceeds via the following steps:

1. nucleation of SiC crystallites in fibre,
2. growth of SiC crystallites accompanied by the generation of SiO and CO,
3. diffusion of SiO and CO from the core to the fibre surface, and
4. diffusion of SiO and CO from the fibre surface to the bulk gas phase.

The kinetic analysis showed that the rate-determining step of the pyrolysis was step 2 [8, 9, 12]. The kinetics were described by an Avrami–Erofeev formula [15]:

$$-\ln(1 - X) = k't^m \quad (2)$$

where k is a rate constant, and m is a parameter which is a function of the reaction mechanism, nucleation rate and geometry of the nuclei. X is the decomposed fraction of Nicalon and is given by Equation 3.

$$X = \Delta W_t/\Delta W_f \quad (3)$$

ΔW_t is the mass loss at some time t, and ΔW_f is the final mass loss after completion of pyrolysis. By taking algorithms of Equation 2, the following equation is introduced.

$$\ln[-\ln(1 - X)] = \ln k + m \ln t \quad (4)$$

Fig. 13 shows the application of rate, Equation 4, to the kinetic data shown in Fig. 1. The plots of $\ln[-\ln(1 - X)]$ versus $\ln t$ give straight lines, and the mean value of m is estimated to be 1.4 from the slopes. This value is nearly equal to $m = 1.5$ obtained when the nuclei growth model satisfies the following conditions: zero nucleation rate, diffusion-control and three-dimensional growth [15].

On the other hand, the kinetic data in N_2 does not obey an Avrami–Erofeev formula. Therefore, the pyrolytic rate in N_2 is controlled by a step other than step 2. AES analysis suggests that Nicalon picks up nitrogen and that a nitrided case is formed during heat treatment in N_2 (Figs 9 to 12). The coarse-grained case (Fig. 7f) is considered to be produced by the pyrolysis of the nitrided case. Nitrogen pick-up compensates the mass loss caused by the pyrolysis, as shown in Fig. 1. The nitrided case is considered to suppress the pyrolysis because of the restricted generation of the pyrolytic gases, SiO and CO, as discussed

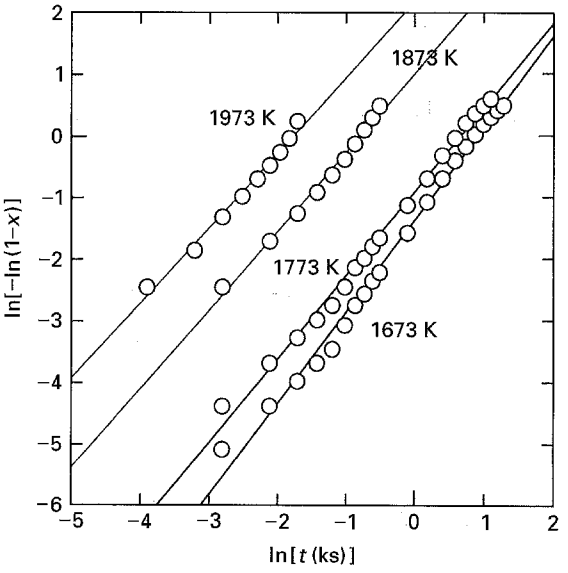

Figure 13 Application of Avrami–Erofeev equation to rate data shown in Fig. 1.

later. This is substantiated by the results of XRD (Figs 3 to 5) and of the tensile test (Fig. 8). The suppression of the pyrolysis also decreases the mass loss in N_2.

The nitrided case is formed by the reaction of N_2 with SiO, CO or β-SiC, the pyrolytic products of Nicalon. First of all, Si_3N_4 is presented as the reaction product between Nicalon and N_2. Nicalon may be roughly regarded as SiC fibre. The reaction between SiC and N_2 results in the formation of Si_3N_4 under one atmospheric pressure of N_2 ($p_{N_2} = 1.01 \times 10^5$ Pa) and below 1728 K, from thermodynamical calculation.

$$3SiC(s) + 2N_2(g) = Si_3N_4(s) + 3C(s) \quad (5)$$

$$\Delta G^\circ(J\ mol^{-1}) = -504670 + 292.1T(K)$$

There is also the possibility that Si_3N_4 is formed by the gas-phase reaction

$$3SiO(g) + 3CO(g) + 2N_2(g) = Si_3N_4(s) + 3CO_2(g). \quad (6)$$

CO_2 is converted into CO by a solution loss reaction.

$$CO_2(g) + C(s) = 2CO(g) \quad (7)$$

The combination of Reactions 6 and 7 gives the following overall reaction.

$$3SiO(g) + 3C(s) + 2N_2(g) = Si_3N_4(s) + 3CO(g) \quad (8)$$

$$\Delta G^\circ(J\ mol^{-1}) = -754460 + 305.3\ T(K)$$

SiC can also be produced in N_2 by the following reaction:

$$SiO(g) + 2C(s) = SiC(s) + CO(g) \quad (9)$$

$$\Delta G^\circ(J\ mol^{-1}) = -83260 + 4.39\ T(K)$$

The dependence of the equilibrium pressure of SiO of Reactions 8 and 9, p_{SiO} on the temperature is shown in Fig. 14. p_{SiO} was calculated for $p_{SiO} + p_{CO} = 10^4$ Pa ($p_{N_2} = 9 \times 10^4$ Pa) and 10^2 Pa ($p_{N_2} = 9.99 \times 10^4$ Pa). It should be noted that Si_3N_4 is stable below 1680 K ($p_{SiO} + p_{CO} = 10^4$ Pa) and below 1740 K ($p_{SiO} + p_{CO} = 10^2$ Pa).

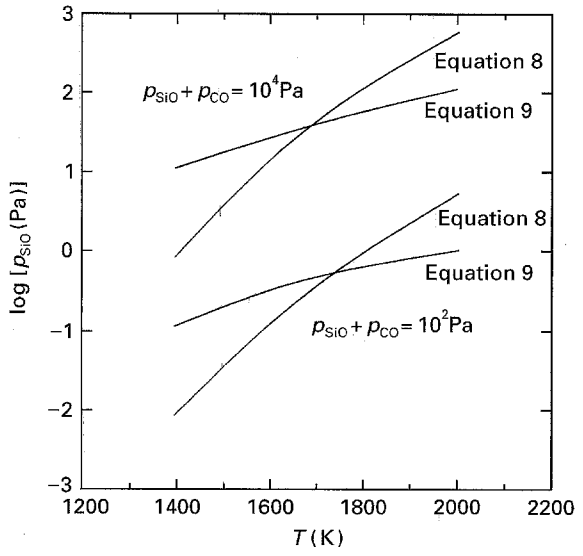

Figure 14 Log p_{SiO} versus temperature diagram for Reactions 8 and 9.

The thermodynamic considerations confirm that the Si_3N_4 layer is not formed on the surface of Nicalon above 1773 K, even though the pyrolysis is suppressed in N_2. Therefore, it is necessary to examine the possibility that the radical bond of silicon with nitrogen is produced. The pyrolytic reaction probably involves a radical mechanism. Both the SiO and CO gases evolved during pyrolysis arise from the radical breakage of ≡Si–O–Si≡ and ≡Si–O–C≡ bonds in Nicalon:

≡Si–O–Si≡ and
≡Si–O–C≡ → ≡Si + SiO(g) + CO(g) (10)

It is considered that a radical ≡Si reacts with N_2 to form the ≡Si–N= bond.

$$\equiv Si + N_2(g) \rightarrow \equiv Si\text{–}N= \quad (11)$$

The ≡Si–N= bonds are considered to form the nitrided case around Nicalon.

When Nicalon is perfectly surrounded by the nitrided case, the pyrolysis proceeds via the following steps:

1. nucleation of SiC crystallites in fibre,
2. growth and coarsening of SiC crystallites accompanied by the generation of SiO and CO,
3. diffusion of SiO and CO from the core to the nitrided case,
4. diffusion of SiO and CO through the nitrided case, and
5. diffusion of SiO and CO from the fibre surface to the bulk gas phase.

The retardation of the pyrolysis in N_2 suggests that the nitrided case restricts the outward transport of the pyrolytic gases, SiO and CO. Therefore, the pyrolytic reaction in N_2 may be controlled by step 4 or by both steps 1 and 4. As a result, this layer prevents the growth of β-SiC crystallites and the reduction in the tensile strength of Nicalon.

When the crystal size of the polycrystalline ceramics is small, its tensile strength is given by the equation [16]

$$\sigma = a + b \cdot d^{-1/2} \quad (12)$$

where d is the mean diameter of the crystal, and a and b are constants. This equation is equivalent to the Hall–Petch formula which is applied to the yield strength of metals. Fig. 15 indicates the applicability of this equation to the strength of Nicalon heated in Ar or N_2. The plots approximately satisfy Equation 12. It may be noted that nearly identical strengths are achieved for the same crystal sizes, regardless of the heat-treatment atmosphere.

The nitrided case is effective for the suppression of pyrolysis only under a N_2 atmosphere. Therefore, the change in atmosphere from N_2 to Ar leads to severe pyrolysis particularly at elevated temperatures, as shown in Fig. 2. As reported previously [17–19], an oxide film also suppressed the pyrolysis of the core under an O_2 atmosphere. Unlike the nitrided case, the oxide film nearly completely prevented the pyrolysis of the core under an Ar atmosphere. When the fibres were subsequently heated in Ar, the nitrided case had

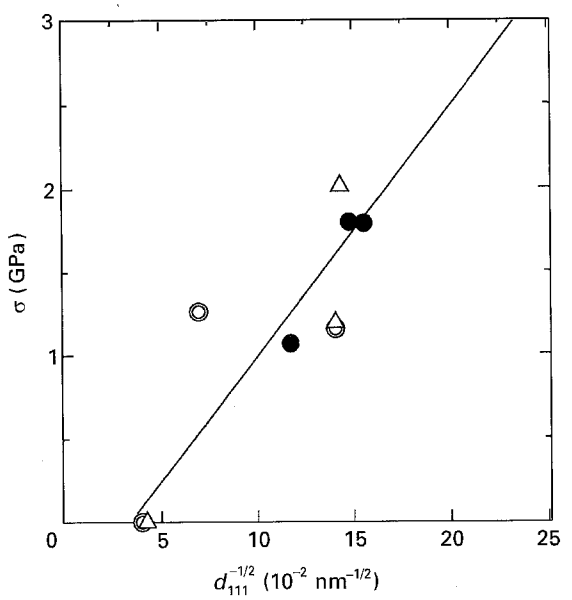

Figure 15 Relation between tensile strength of Nicalon and reciprocal square root of SiC crystal size. Key: ● N_2; (◎) Ar; △ $N_2 \rightarrow$ Ar.

a tendency to disappear gradually (Fig. 12), although the oxide film was retained for long periods [16–18].

5. Conclusion

The pyrolytic behaviour of Nicalon was investigated in both N_2 and Ar at temperatures from 1673 to 1973 K. The following results were obtained.

1. The pyrolytic rates were smaller in N_2 than in Ar. For the fibre heated in N_2, crystallization to β-SiC was retarded and the tensile strength was maintained at a high level. This fibre retained 42% of its original strength even at 1873 K.

2. AES analysis showed nitrogen pick-up on the surface of the fibre heat treated in N_2. The nitrided case was effective in retarding the pyrolysis of the core in N_2, but not in Ar.

3. In Ar, the pyrolytic rates obey an Avrami–Erofeev formula and is considered to be controlled by the growth of β-SiC crystals. In N_2, the diffusion of SiO and CO through the nitrided case is the rate-controlled step of the pyrolysis.

4. The strength was inversely proportional to the square root of the β-SiC crystal size, regardless of the heat treatment atmosphere.

References

1. T. MAH, N. L. HECHT, D. E. McCULLUM, J. R. HOENIGMAN, H. M. KIM, A. P. KATZ and H. A. LIPSITT, *J. Mater. Sci.* **19** (1984) 1191.
2. A. S. FAREED, P. FANG, M. J. KOCZAK and F. M. KO, *Amer. Ceram. Soc. Bull.* **66** (1987) 353.
3. S. M. JOHNSON, R. D. BRITTAIN, R. H. LAMOREAUX and D. J. ROWCLIFFE, *ibid.* **71** (1988) C132.
4. M. H. JASKOWIAK and J. A. DiCARLO, *ibid.* **72** (1989) 192.
5. H.-E. KIM and A. J. MOORHEAD, *ibid.* **74** (1991) 666.
6. B. A. BENDER, J. S. WALLACE and D. J. SCHRODT, *J. Mater. Sci.* **26** (1991) 970.
7. G. S. BIBBO, P. M. BENSON and C. G. PANTANO, *ibid.* **26** (1991) 5075.
8. T. SHIMOO, M. SUGIMOTO and K. OKAMURA, *Nippon Kinzokugakkaishi* **54** (1990) 802.
9. *Idem., Seramikkusu Ronbunshi* **98** (1990) 1324.
10. T. SHIMOO, M. SUGIMOTO, Y. KAKEHI and K. OKAMURA, *Nippon Kinzokugakkaishi* **55** (1991) 294.
11. *Idem., Seramikkusu Ronbunshi* **99** (1991) 401.
12. T. SHIMOO, H. CHEN and K. OKAMURA, *J. Ceram. Soc. Jpn.* **100** (1992) 48.
13. *Idem, ibid.* **100** (1992) 929.
14. T. SHIMOO, Y. KAKEHI, K. KAKOMOTO and K. OKAMURA, *Nippon Kinzokugakkaishi* **56** (1992) 175.
15. S. F. HULBERT, *J. Br. Ceram. Soc.* **6** (1969) 11.
16. K. HAMANO and S. KIMURA, "Fundamental Science of Fine Ceramics", (Asakurashoten, Tokyo) (1990) p. 98.
17. T. SHIMOO, H. CHEN, K. KAKIMOTO and K.OKAMURA, *J. Ceram. Soc. Jpn.* **101** (1993) 295.
18. T. SHIMOO, H. CHEN and K. OKAMURA, *Nippon Kinzokugakkaishi* **57** (1993) 652.
19. *Idem, J. Mater. Sci.* **29** (1994) 456.

Received 1 August 1994
and accepted 1 December 1995